Ordered Structures in a Series of Liquid Crystalline Poly(ester imide)s

Ricardo Pardey, Dexing Shen, Patricia A. Gabori, Frank W. Harris, and Stephen Z. D. Cheng*

Institute and Department of Polymer Science, The University of Akron, Akron, Ohio 44325-3909

Jerry Adduci and John V. Facinelli

Department of Chemistry, Rochester Institute of Technology, Rochester, New York 14623-0887

Robert W. Lenz

Department of Polymer Science and Engineering, University of Massachusetts, Amherst, Massachusetts 01003

Received February 8, 1993; Revised Manuscript Received April 12, 1993

ABSTRACT: A series of poly(ester imide)s (PEIMs) has been synthesized from *N*-[4-(chloroformyl)phenyl]-4-(chloroformyl)phthalimide and different diols with methylene units of 4 to 12 (*n*). PEIMs with both even and odd methylene units exhibit a monotropic mesophase behavior during cooling due to the supercooling necessary for crystallization. Identification of this mesophase as a monotropic liquid crystal with smectic A order has been carried out via differential scanning calorimetry, wide angle X-ray diffraction (WAXD), small angle X-ray scattering, polarized light microscopy, and transmission electron microscopy. It is found that the methylene units in these chain molecules are also largely responsible for the formation of this liquid crystal phase. After investigating different types of main chain mesogen–nonmesogen liquid crystal polymers, a general concept considering the contributions to enthalpy and entropy changes during the liquid crystal transitions may be associated with the relative rigidity, linearity, and regularity of the mesogenic groups compared to the methylene units. Detailed WAXD study of fiber and powder patterns indicates that the degree of orientation and the order correlation lengths along and perpendicular to the direction of chain molecules (chain lateral packing and layer structure) not only increase with the number of methylene units but also show an even–odd alternation. A possible chain packing model is suggested. The morphology and defects of this smectic A liquid crystal phase are also discussed.

Introduction

Recently, it has been reported that thermotropic poly(ester imide)s [PEIM(*n*)s] with both even ($n = 4$) and odd ($n = 9$) methylene units show monotropic mesophase behavior, which was identified as a liquid crystal.[1] This monotropic phase is only metastable at temperatures below the crystal melting temperature (T_d). Experimentally, the monotropic phase can be observed on cooling provided that the crystallization process is bypassed due to supercooling. Recognition of monotropic phases can be traced as far back as 1877[2] and has been widely reported in small molecule liquid crystals as early as 1923.[3] For thermotropic liquid crystal polymers, as an example, a series of polyethers synthesized from 1-(4-hydroxyphenyl)-2-(2-methyl-4-hydroxyphenyl)ethane and α,ω-dibromoalkanes with the odd-numbered methylene units [MBPE(*n*=odd)s], has been reported to show monotropic behavior.[4-12] The thermodynamic consideration of the monotropic liquid crystal phase has been clearly described by Percec and Keller.[13] The general concept is that the Gibbs free energy of the monotropic liquid crystal phase does not possess its own temperature region where this phase is thermodynamically most stable compared with other phases.

In this paper, the ordered structures of a series of PEIMs in which the number of methylene units varies from 4 to 12 are reported. These poly(ester imide)s were synthesized from *N*-[4-(chloroformyl)-phenyl]-4-(chloroformyl)phthalimide and the respective diols by solution polymerization in refluxing 1,2,4-trichlorobenzene (TCB). The chemical structures of the repeat units are

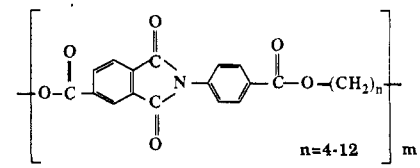

It should be noted that in this series of PEIMs the mesogenic group is asymmetric. The sequences of head-to-head and heat-to-tail are randomly distributed along the chain molecules. This series of PEIMs has the same chemical structures as a family of those synthesized by Kricheldorf et al.,[14-19] but with a different synthetical route. They found that PEIM(*n*=even)s form a crystalline state, a layered supermolecular ordered "crystalline smectic state", and a smectic glass. PEIM(*n*=odd)s crystallize much more slower and the isotropic glasses can be obtained. After crystal melting, all PEIMs exhibit the isotropic state.[16,18] In their structure model, mesogenic groups and methylene units were proposed to be tilted in uniaxially oriented samples to explain the wide-angle X-ray diffraction (WAXD) fiber patterns.[18] It should be noted that in main mesogen–nonmesogen liquid crystal polymers smectic phases were observed only in a very few cases. A recent review including this topic was given by Noel,[20] where he summarized the works from Ober and Lenz,[21] Roviello and Sirigu,[22] Frosini and Marchetti,[23] Thierry et al.,[24] and his own research group.

Based on the work of Kricheldorf et al. and our own study previously reported, we focus on the identification

* To whom the correspondence should be addressed.

0024-9297/93/2226-3687$04.00/0

Table I. Inherent Viscosities of PEIM Polymers[a]

PEIM(n)	η_{inh} (dL/g)	PEIM(n)	η_{inh} (dL/g)
4	0.40	9	0.62
5	0.50	10	0.61
6	0.52	11	0.60
7	0.65	12	0.59
8	0.60		

[a] The inherent viscosities were measured in m-cresol at 303 K at a concentration of 0.5%.

of the ordered structure in this series of PEIMs. In particular, we try to understand what kind of ordered structure exists and what the effect of the even–odd alternation does in the monotropic liquid crystal state. Molecular packing, morphology, and defects of the liquid crystal phase in this series of PEIMs are also discussed.

Experimental Section

Materials and Samples. The synthesis of PEIMs involved the coupling of *N*-[4-(chloroformyl)phenyl]-4-(chloroformyl)-phthalimide with respective diols by solution polymerization in refluxing 1,2,4-trichlorobenzene (TCB). The detailed procedure has been described in a recent publication.[1] Inherent viscosity measurements were carried out in m-cresol at 303 K, and the results are listed in Table I. Differential scanning calorimetry (DSC) experiments used a typical sample weight of 5 mg. For fast cooling measurements, the sample weight decreases correspondingly to avoid thermal lag. PEIM fibers were melt-spun and quenched to below their glass transition temperatures in order to retain their liquid crystal structures in the fibers. The fiber diameters were about 20 μm and the elongation ratios around 10. Bulk samples for powder WAXD and small angle X-ray scattering (SAXS) experiments were prepared by compressing the samples under pressure at high temperatures to form films with a thickness of about 0.5 mm. Solution cast films were used for polarized light microscopy (PLM) and transmission electron microscopy (TEM) observations. The solvent was evaporated in a vacuum oven at 520 K for 5 h. Solid films with a thickness of about 10 μm were obtained.

Wide Angle X-ray Diffraction (WAXD). A Rigaku X-ray generator with a 12-kW rotating anode was coupled with a hot stage. The Cu Kα incident beam is point-focused and monochromatized. The temperature controller is within ±1 K precision. Quenched samples from the isotropic melt were measured at room temperature, and nonisothermal experiments of PEIM(n) powder patterns were conducted at both heating and cooling rates of 5 K/min. The scanning region of 2θ ranges from 2° to 50°. The quenched (as-spun) fiber patterns were obtained with a Siemens two-dimensional area detector. The d-spacing was calibrated using a silicon powder with a $2\theta = 28.46°$. The diffraction peak positions and widths from both transmission and reflection modes of WAXD experiments were carefully calibrated.

Small Angle X-ray Scattering (SAXS). Time-resolved synchrotron small angle X-ray scattering (SAXS) experiments were carried out at the Oak Ridge National Laboratory beam line X-14 at the National Synchrotron Light Source (NSLS). The X-ray wavelength was 0.15498 nm (8.000 keV). A positional sensitive proportional counter (Ordella 1020) was used to record the scattering patterns. A home-made temperature-jumping hot stage was built and situated on a Huber goniometer for isothermal measurements. The temperature of this hot stage was calibrated with standard materials during the beam radiation. The precision of the temperature controller was ±0.5 K. Lorentz correction was made by multiplying the intensity, I (counts per second), with s^2 ($s = 2 \sin\theta/\lambda$, where λ is the wavelength of the synchrotron X-ray radiation).

Differential Scanning Calorimetry (DSC). Since the liquid crystal transition is monotropic,[1] different cooling rates ranging from 0.31 to 80 K/min were used to characterize the first-order transition behavior using a Perkin-Elmer DSC-2. The DSC was calibrated by using standard materials for its temperature and heat flow scales at different heating rates. The weight of DSC pans used were controlled within an accuracy of ±0.005 mg.

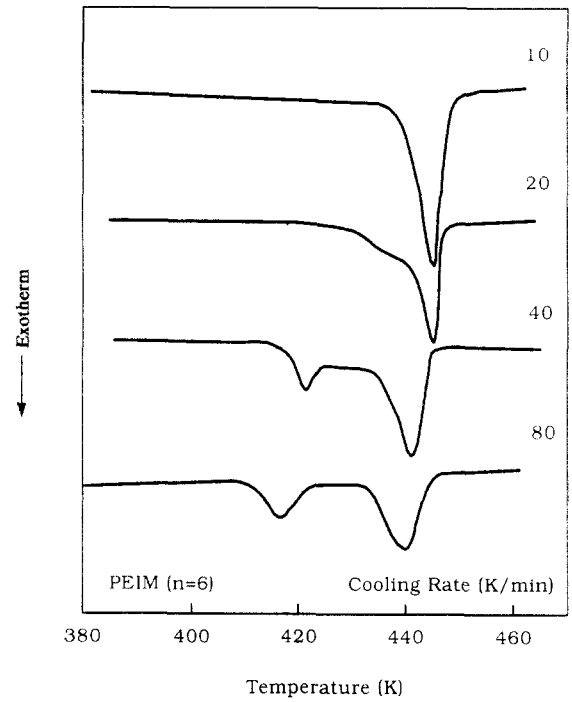

Figure 1. Set of DSC curves for PEIM(n=6) cooling from the isotropic melt at different cooling rates.

Polarized Light Microscopy (PLM). The liquid crystal morphologies of PEIMs were observed via an Olympus HB-2 microscope coupled with a Mettler FP-82 hot stage. The PEIM samples were also mechanically sheared between two glass slides slightly below their mesophase transition temperatures. These sheared samples were then quenched to below their glass transition temperatures to observe the banded texture.

Transmission Electron Microscopy (TEM). Liquid crystal defect observations were carried out through a JEOL JEM-120U microscope at an accelerating voltage of 100 kV. The samples were prepared in the same way as in the case of PLM experiments, and then were physically oversheared to separate the glass slides and immediately quenched. The samples were reheated to a temperature 10–20 °C below the mesophase transition temperature for further crystallization. The crystallization temperature was carefully selected since one needs to retain the chain orientation induced during shearing, and therefore, lamellar crystals can grow to ensure that the lamellar crystal direction is approximately normal to the chain orientation. This method is known as the "lamellar decoration method", and it was first proposed by Thomas et al.[25-27] to identify the liquid crystal polymer texture. The samples were then coated by heavy metals (Au/Pt 0.4/0.6, 30° tilted to the sample surface) and carbon (90° to the sample surface). Finally, the PEIM samples were dissolved in a mixed solvent of trifluoroacetic acid and chloroform, and the replicas were picked up on TEM grids in acetone. In order to determine the chain molecular direction, the sheared and coated samples were also directly examined by electron diffraction experiments under the TEM.

Results and Discussion

Thermal Transition Behavior. Figure 1 shows a set of DSC cooling curves of PEIM(n=6) from the isotropic melt to below its glass transition at different cooling rates. It is interesting to find that the onset temperature of the first-order transition exothermic peak (448.9 K) is almost cooling rate independent, as well as its heat of transition (6.1 kJ/mol). Further cooling leads to a second exothermic peak. However, this second peak exhibits supercooling dependence in both temperature and heat of transition. A similar transition behavior can also be observed in all

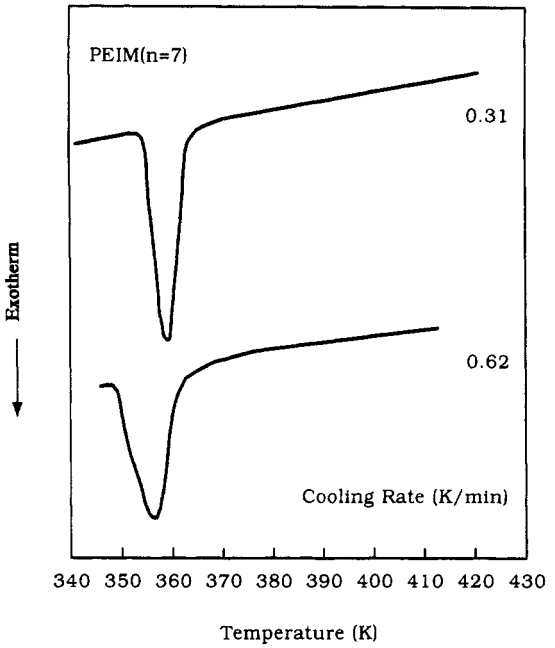

Figure 2. Set of DSC curves for PEIM(n=7) cooling from the isotropic melt at different cooling rates.

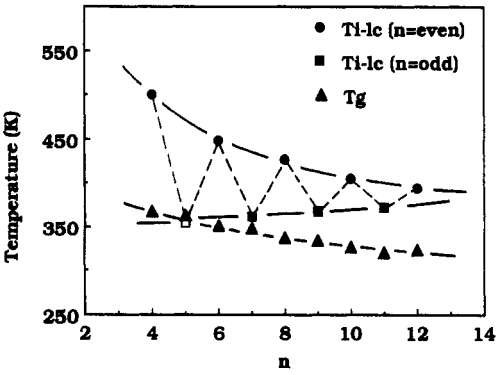

Figure 3. Relationships of the onset transition temperature of the exothermic peak and glass transition temperatures with the number of methylene units.

PEIM(n=even) polymers. On the other hand, only one exothermic peak can be seen for all PEIM(n=odd) polymers during cooling, as shown in Figure 2 for PEIM-(n=7), as an example. This peak is cooling rate independent in both the transition temperature (361.0 K) and the heat of transition (3.5 kJ/mol). Only very slow cooling rates can be applied (<1 K/min) due to the slow transition kinetics. It should be noted that for PEIM(n=5) no exothermic process can be found during cooling even at a very slow cooling rate (such as 0.31 K/min). This is because the glass transition temperature of PEIM(n=5) is at 365 K, and the first-order transition temperature during cooling is expected to be very close to the T_g (see below, Figure 3). The cooling rate independence should generally be an indication that the transition is close to a thermodynamic equilibrium, and therefore, this behavior is typical for a liquid crystal transition.

If one extrapolates the transition temperature and the heat of transition of the first exothermic peak observed during cooling to a rate of 0 K/min, the thermodynamic properties of this series of PEIMs are shown in Figures 3–5, where the transition temperature, the transition enthalpy and transition entropy changes are plotted with respect to the number of methylene units. It is evident that these figures illustrate an even–odd alternation on these thermodynamic properties. Interestingly enough, the transition temperature of PEIM(n=even) decreases,

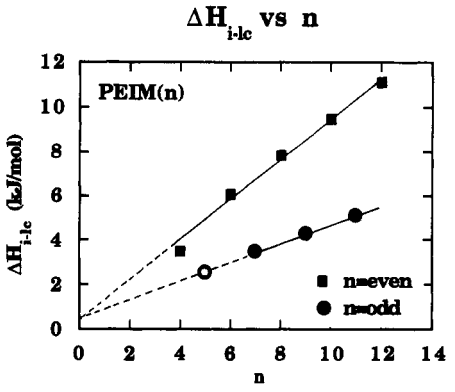

Figure 4. Relationship between the enthalpy change of the exothermic peak and the number of methylene units.

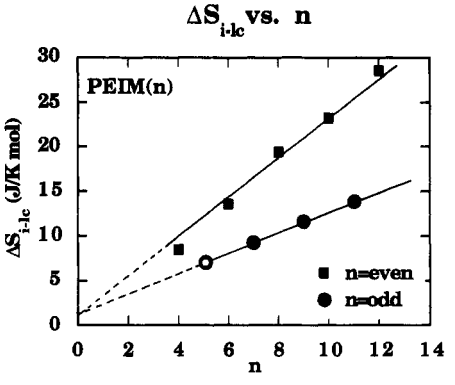

Figure 5. Relationship between the entropy change of the exothermic peak and the number of methylene units.

while that of PEIM(n=odd) increases with increasing the number of methylene units, as shown in Figure 3. Glass transition temperatures of PEIMs are also included in Figure 3 for complete information. When the transition temperature is close to the glass transition temperature, the transition kinetics becomes extremely slow because of a reduction in chain mobility.

Figures 4 and 5 indicate linear relationships between the enthalpy and entropy changes with the number of methylene units. Following the method proposed by Blumstein and Thomas[28] and Blumstein and Blumstein,[29,30] extrapolations of these linear relationships to n = 0 yield small values of the enthalpy and entropy changes, which should represent the contributions from the mesogenic group. It is surprising that the extrapolated values for PEIM(n=even)s and PEIM(n=odd)s are close to each other, and they are 0.58 kJ/mol and 1.35 J/(K mol), respectively, which are on the lower boundaries of the enthalpy and entropy changes of small molecule liquid crystals to the isotropic melt.[9] Such small values may be the cause of geometrical asymmetry of the mesogenic groups and random chemical connections of head-to-head and head-to-tail configurations, which could lead to a packing difficulty compared to the regular main chain mesogen–nonmesogen type of liquid crystal polymers. On the other hand, the slopes of linear lines for both PEIM-(n=even)s and -(n=odd)s should be attributed to the contributions of each methylene unit to the orientational order in the liquid crystal phase. The enthalpy changes are 0.80 kJ per mole of methylene units for PEIM(n=even)s and 0.40 kJ per mole of methylene units for PEIM-(n=odd)s, while the corresponding entropy changes are 2.30 kJ/(K mol) and 1.07 J/(K mol), respectively. This may be an indication that in the liquid crystal state of PEIM(n), the methylene units also significantly contribute to the orientational order. A deviation of the data on

Table II. Enthalpy and Entropy Changes Contributed by Mesogenic Groups and Methylene Units in ME9-Sns, MBPE(n=odd)s, and PEIMs

samples	ΔH_i (kJ/mol)	ΔS_i (J/(K mol))
ME9-Sn[a]		
even		
mesogen	4.7	7.55
methylene	0.16	0.87
odd		
mesogen	0.94	1.41
methylene	0.19	0.57
MBPE(n=odd)s[b]		
mesogen	0.11	1.30
methylene	0.64	1.90
PEIM		
even		
mesogen	0.58	1.35
methylene	0.80	2.30
odd		
mesogen	0.58	1.35
methylene	0.40	1.07

[a] The data are from refs 23–25. [b] The data are from ref 9.

PEIM(n=4) from the linear relationships may be caused by the relatively low molecular weight of this polymer (relatively lower inherent viscosity, see Table I).

Along this line, these values can be compared with two other examples. For a set of regular main chain mesogen–nonmesogen type of liquid crystal polymers synthesized from (4,4′-dihydroxy-2,2′-dimethylazoxybenzene)alkanedioic acid (ME9-Sn)[28–30] and a set of polyethers, [MBPE(n=odd)s],[9] their enthalpy and entropy changes contributed by both mesogenic groups and methylene units are listed in Table II, as well as the data from PEIMs. As illustrated in this table, one can separate these data into two groups, each has respective even- or odd-numbered methylene units. For the odd-numbered methylene units, it seems that the methylene units in MBPE(n=odd)s show the most ordered structure, which has the highest enthalpy and entropy changes during the transitions, followed by those in PEIM(n=odd)s. The methylene units in ME9-Sn(n=odd)s possess the least ordered structure. Only two sets of data for the even-numbered methylene units are available. The methylene units in PEIM(n=even)s are more ordered compared to those in ME9-Sn(n=even)s. On the other hand, the order contribution sequence from the mesogenic groups is exactly opposite, namely, the mesogenic groups in ME9-Sn show the highest contribution to the enthalpy and entropy changes, while those contributions in MBPEs are the lowest. It should be noted that MBPEs have the semiflexible mesogenic groups, PEIMs, the asymmetric mesogenic groups with random chemical connections, and ME9-Sn, the regular mesogenic groups. The former two polymers only exhibit monotropic liquid crystal behavior, and the latter, an enantiotropic one. It seems to us that the contributions to the thermal transition behavior are associated with relative linearity, rigidity, and regularity of the mesogenic groups with respect to the methylene units. These two portions in the repeating units may possess a balance of these contributions from each other. Regular, rigid, linear mesogenic groups should be easier to form more ordered packing by sacrificing the packing in methylene units compared to irregular and even semiflexible mesogenic groups. These mesogenic groups in MBPEs and PEIMs may have to partially rely on the packing in methylene units since less orientationally ordered structures for themselves can be achieved. However, a quantitative analysis has to be postponed until a broader base in the study of main chain mesogen–nonmesogen type liquid crystal polymers is obtained.

Identification of the Ordered Structure. From their thermal transition behavior, it is clear that PEIMs possess a liquid crystal transition during cooling. Further identification of the ordered structure is necessary to clasify this liquid crystal phase in PEIM polymers. Figure 6 shows a series of WAXD fiber patterns for PEIMs. Overall, along the equatorial direction, the fiber patterns only show a pair of diffused spots. This indicates that the lateral packing of chain molecules in the fibers is liquid-like. No long range lateral order is preserved. The diffused spots along the equatorial direction also possess different degrees of orientation for PEIM(n=even)s and -(n=odd)s based on the arc shape of the spots. However, along the meridian direction, sharp diffraction spots are obvious. With increasing the number of methylene units, the number of the diffractions along the meridian direction increases with an even–odd alternation. This is clear evidence that the layer structure exists in these quenched PEIM samples. No diffraction spots can be found in quadrants, revealing that three-dimensional long range order is not formed in these polymers.

When one uses azimuthal angular integration to calculate the degree of orientation (orientation factor) along the equatorial direction, S_e, which is representative of the orientation in the chain molecules along the lateral packing direction, Figure 7 illustrates the orientation factor change with respect to the number of methylene units. One observes that, first, with increasing the number of methylene units the degree of orientation improves. Second, the orientation factor also exhibits an even–odd alternation. The PEIM(n=even) possesses about a 10–20% higher degree of orientation order compared to its neighboring PEIM(n=odd)s. This reveals that within the layer structure the chain molecules, in particular, the mesogenic groups in PEIM(n=even)s should have a better orientation along the lateral packing direction compared to those in PEIM(n=odd)s. The maximum intensity of those diffused spots is always on the equatorial direction, indicating that the vectors of chain molecules (in particular, the mesogenic groups) are basically parallel to the fiber axis. On the other hand, one can experimentally obtain the orientation factor along the meridian direction, S_m, which represents the orientation of the layer structure, as shown in Figure 8. It is interesting that an even–odd alternation of the orientation factor also exists. Generally speaking, this factor is about 10–15% higher compared to that along the equatorial direction (S_e) for the same fiber sample. The maximum intensity of the layer diffraction spots is always on the meridian direction, giving evidence that the normal vectors of the layer surfaces are basically parallel to the fiber axis. Both phenomena can be explained by the different conformations of methylene units in the polymers. It has been reported, from a theoretical point of view, that in main chain mesogen–nonmesogen type of liquid crystal polymers the even-numbered methylene units provide better orientational correlation between consecutive mesogenic groups along the chain direction compared with the odd-numbered methylene units.[31–33]

The scanning intensities of the WAXD fiber patterns (Figure 6) along both the equatorial and meridian directions provide widths at half-height of the diffraction peaks which are reciprocally proportional to the order correlation lengths, ζ_e and ζ_m, along these directions. They can be calculated by using the Shrerrer equation as a first approximation. It is clear that not only an even–odd alternation can be found in both correlation lengths but also they increase with the number of methylene units, as shown in Figures 9 and 10. The correlation lengths along

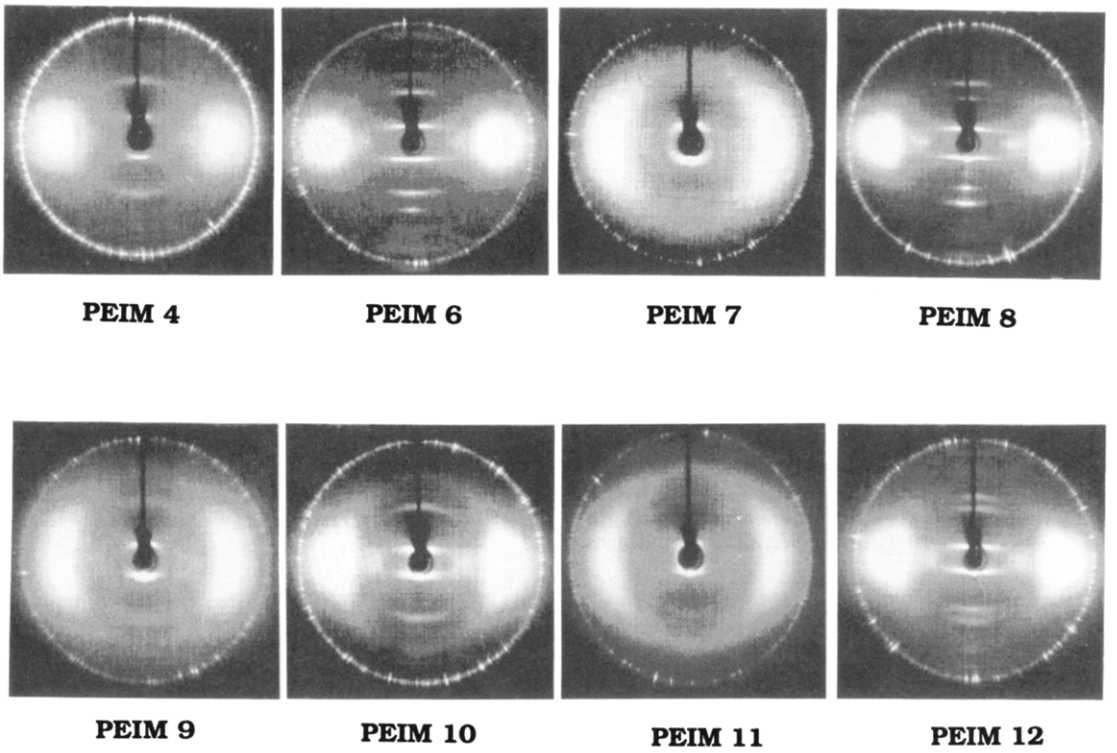

Figure 6. Set of WAXD fiber patterns for PEIMs.

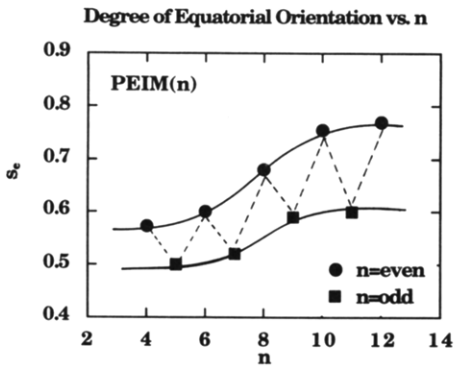

Figure 7. The orientation factor along the equatorial direction of the fiber patterns, S_e, changes with the number of methylene units.

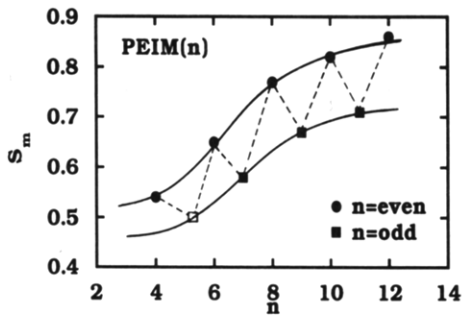

Figure 8. Orientation factor along the meridian direction of the fiber patterns, S_m, changes with the number of methylene units.

the meridian direction are about one order of magnitude higher than those along the equatorial direction. This manifests that the layer orientation along the chain molecular direction (fiber axis) shows a quasi long range order, while the lateral packing shows a short range order. This result is qualitatively consistent to the observations of smectic A phase in small molecule liquid crystals and side-chain liquid crystal polymers.[34] Quantitatively, however, the values observed here are lower than those of small molecule liquid crystals and even those of side-chain

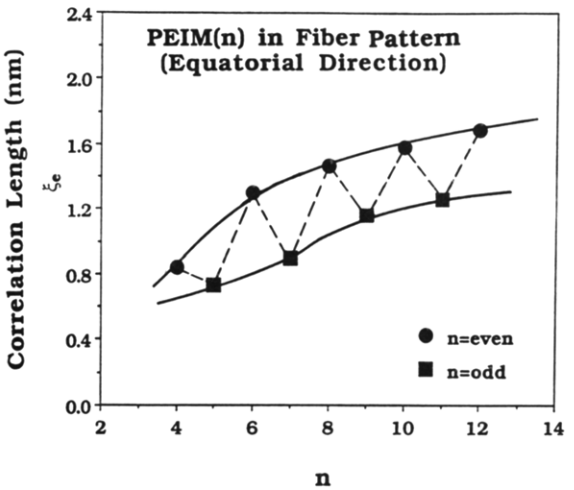

Figure 9. Relationship between the order correlation length, ζ_e, and the number of methylene units in WAXD fiber patterns.

liquid crystal polymers. This reveals that in main-chain mesogen–nonmesogen type of liquid crystal polymers such as PEIMs, the orientation order is hampered by the causes of less mesogenic group mobility due to the connectivities with methylene units and chain entanglements.

When one further investigates the layer spacing along the meridian direction from the fiber patterns, it is evident that the layer spacing increases with the number of methylene units with a clear even–odd alternation (Figure 11). Extrapolations of both layer spacings to $n = 0$ yield 1.43 nm for PEIM(n=even)s and 1.26 nm for PEIM(n=odd)s. The value of 1.43 nm is very close to the mesogenic groups length along an extended conformation based on computer modeling.[35] This indicates, again, that in PEIM(n=even)s the vector of mesogenic groups is perpendicular to the layer surface. However, the value of 1.26 nm for the mesogenic groups in PEIM(n=odd)s is smaller compared to the calculated value. One may invoke the explanation that the vector of mesogenic groups in the liquid crystal phase is tilted with respect to the layer surface

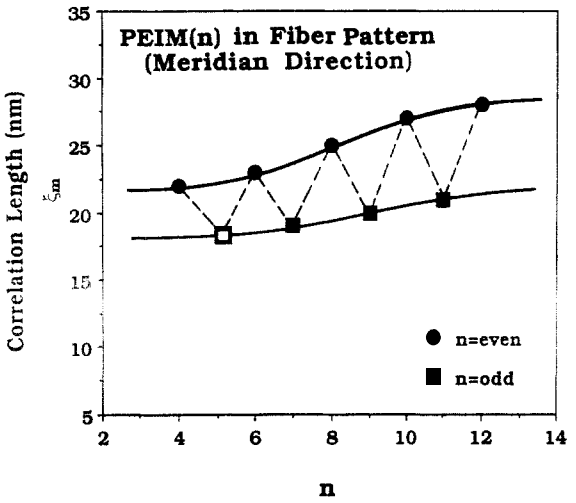

Figure 10. Relationship between the order correlation length, ζ_m, and the number of methylene units in WAXD fiber patterns.

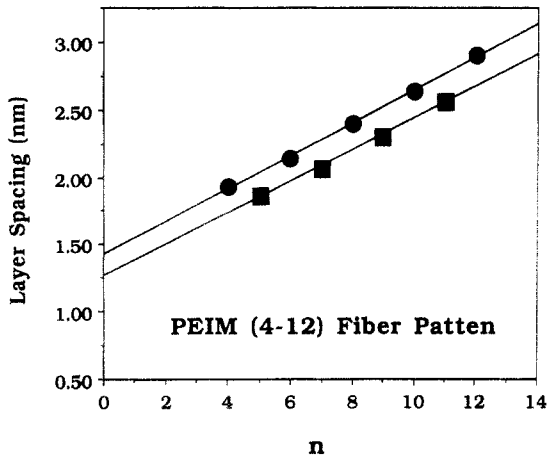

Figure 11. Relationship between the layer spacings and the number of methylene units in PEIMs.

for PEIM(n=odd)s. Two possibilities could be speculated: tilting the vector of chain molecules and tilting the normal vector of layer surfaces with respect to the fiber axis. As a result, one has to observe either the tilted X-ray diffraction(diffused) spots along the equatorial direction because of the tilted molecules within the layer, while the layer surface is perpendicular to the fiber axis (Figure 12a), or the tilted spots along the meridian direction since the layer structure is tilted to the fiber axis, while the chain molecular direction is parallel to the fiber axis (Figure 12b). However, for both PEIM(n=even)s and -(n=odd)s we do not observe any tilted WAXD diffraction spots along either the equatorial or the meridian directions (Figure 6). Another possibility is that in order to form an orientationally aligned layer structure in PEIM(n=odd)s, one has to sacrifice the lowest rotational potential for methylene units as well as for the C–O bonds in ester groups. This may lead to a shorter length of mesogenic groups which remain to be rigid. However, this speculation can only be confirmed through solid-state nuclear magnetic resonance experiments.

The slopes of both linear lines in Figure 11 are also different, with 0.122 nm/n for PEIM(n=even)s and 0.117 nm/n for PEIM(n=odd)s. These values indicate an average single methylene unit contribution to the layer spacing. Both of them are smaller than the length of projection of a C–C bond in the *trans* conformation along the chain direction (0.127 nm). Therefore, it is also speculated that the methylene units in the layers may involve a certain degree of kinks. In particular, the degree

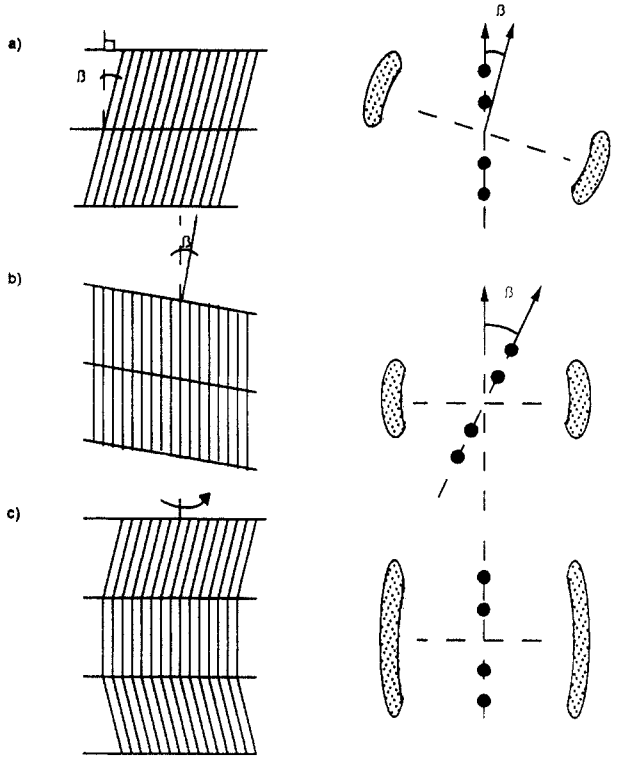

Figure 12. Set of schematic WAXD diffraction patterns for different molecular packings in liquid crystals: (a) tilted vectors of chain molecules; (b) tilted normal vectors of layer surfaces; (c) a broad orientation distribution of the vectors of the chain molecules.[20]

of kinks may be higher in PEIM(n=odd)s than that in PEIM(n=even)s, which results in a smaller value of the slope in Figure 11. This is perhaps the reason why one observes 50% reduction of the contribution in the entropy change for each methylene unit for PEIM(n=odd)s compared to PEIM(n=even)s. Based on all the WAXD experimental observations, one can conclude that PEIMs possess a liquid crystal phase with smectic A order.

If one studies the transition behavior using thermal WAXD method by cooling the powder samples from the isotropic melt, a clear reduction in the d-spacing of the halo around 21° for each PEIM can be observed at the temperature where the first exothermic peak is observed (Figures 1 and 2). Figure 13 manifests the relationships between the d-spacing and temperature for all PEIMs. This reduction of the d-spacing indicates that the lateral chain packing has a measurable change during the transition although no three-dimensional order is formed (no other diffraction peaks can be observed during and immediately after the transition in a 2θ range between 5° and 50°). Interestingly enough, such reduction of the d-spacing becomes deeper with increasing the number of methylene units. This reveals that the longer methylene segment may achieve a better lateral packing by themselves in the liquid crystal state.

On the other hand, WAXD powder patterns of quenched PEIM(n=4–12) polymers to liquid nitrogen also provide ordered structure information. Figure 14 shows these quenched WAXD patterns. It is interesting that all the polymers exhibit a low angle diffraction peak in a 2θ range below 5°. They are representative of the layer structure in the liquid crystal phase. With increasing the number of methylene units, not only the intensity of this peak increases but also the peak position shifts to lower angles. In the wide angle region, the 21°-halos for PEIM(n=even)s are much sharper than those of PEIM(n=odd)s. In certain

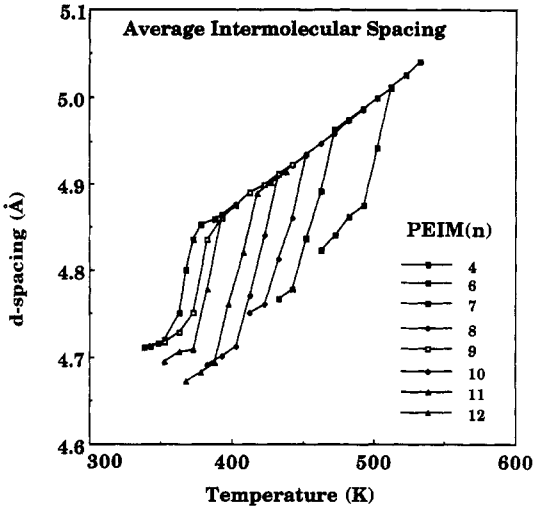

Figure 13. WAXD d-spacings of 21°-halo change with temperature during cooling for PEIMs. The temperatures where the reduction of d-spacing occurs correspond to the exothermic transition temperatures observed in DSC (e.g. see Figures 1 and 2).

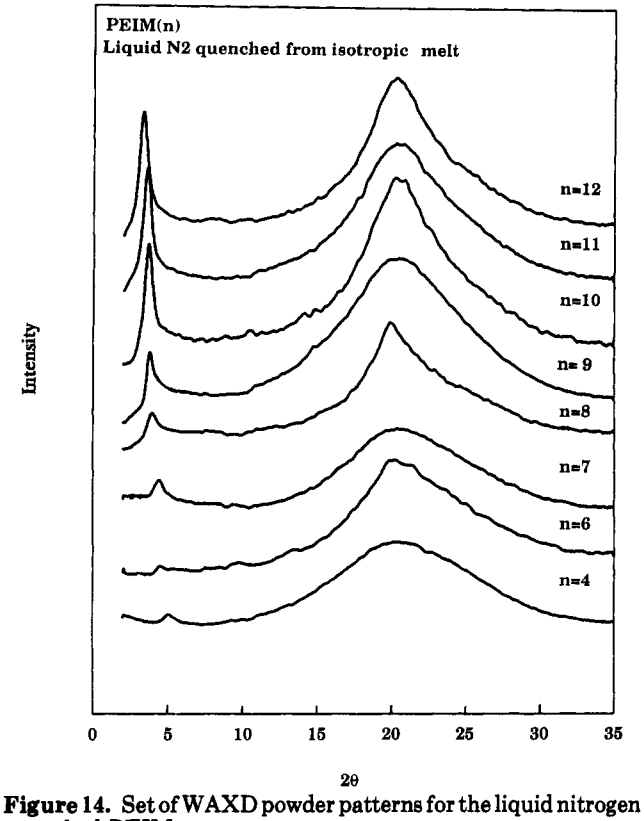

Figure 14. Set of WAXD powder patterns for the liquid nitrogen quenched PEIMs.

cases, the sharpness of this halo may resemble a hexagonal lateral packing in the chain molecules. Further study leads to detailed information about the ordered structure and the order correlation in the liquid crystal phase. Figure 15 is a normalized WAXD intensity of the low angle (<5°) diffraction peak shown in Figure 14 versus the number of methylene units. The normalization process involves the sample thickness and X-ray beam intensity. It is clear that the diffraction intensity increases with n. When n is higher than eight, the intensity increase becomes drastic, and reaches a plateau after n reaches 12. From this figure, one may expect that the layer structure is increasingly developed with increasing n. Furthermore, one may investigate in detail the widths at half-height of the low angle diffraction peak and the 21°-halo in PEIMs, which

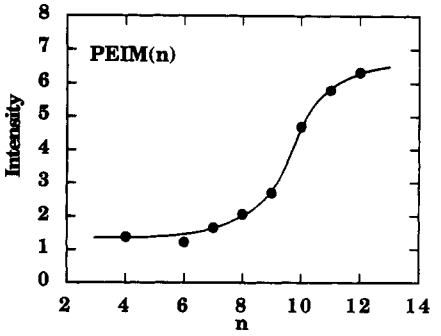

Figure 15. Normalized low angle WAXD diffraction intensities change with the number of methylene units.

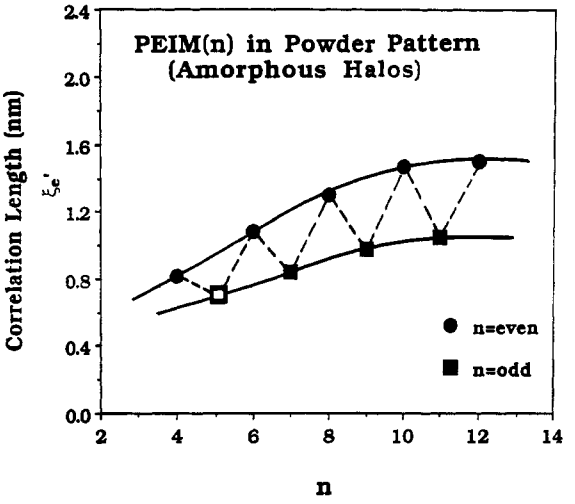

Figure 16. Relationship between the order correlation length, ζ_e', obtained from the 21°-halos and the number of methylene units in the WAXD powder patterns.

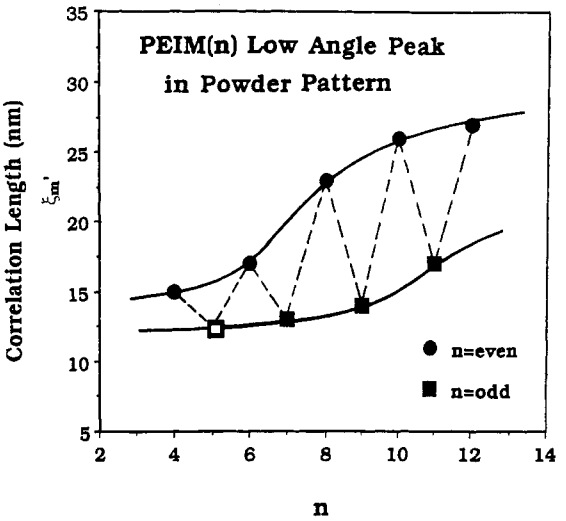

Figure 17. Relationship between the order correlation length, ζ_m', obtained from the low angle peaks and the number of methylene units in the WAXD powder patterns.

provide the order correlation length of the layer structure and lateral packing, respectively. Similar to the cases of PEIM fibers, Figures 16 and 17 show such order correlation lengths, ζ_e' and ζ_m', from powder WAXD patterns of PEIMs. Again, an even–odd alternation is seen in both cases. Interestingly enough, the comparison can be made between the fiber (Figure 10) and powder (Figure 17) WAXD patterns. This reveals that the values of ζ_m obtained from the meridian directions in the fiber patterns for PEIMs with n = 4–9 are substantially higher than those (ζ_m') obtained from the powder patterns. In

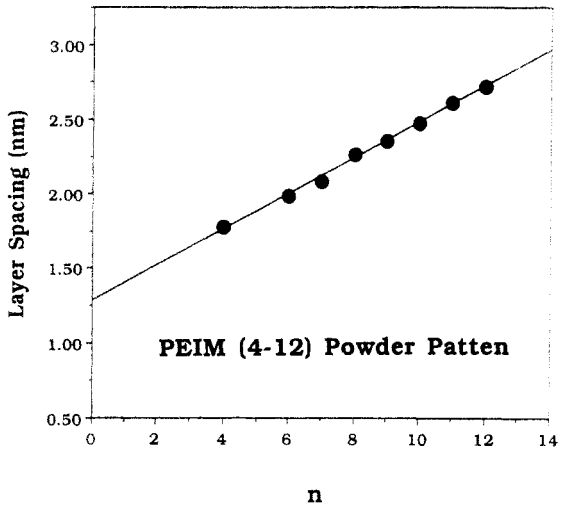

Figure 18. Relationship between the layer spacing of the low angle peak in WAXD powder diffraction and the number of methylene units.

particular, the correlation lengths for PEIM(n=odd)s improve drastically under the uniaxial orientation. With increasing the number of methylene units, the effect of this orientation gradually decreases, such as in the case of PEIM(n=12). On the other hand, a comparison can also be made for the values of ζ_e (Figure 9) and ζ_e' (Figure 16) for the fiber and the powder patterns, which in both cases show short range order. The values obtained from the fiber patterns are about 10% higher than those for the powder patterns for the same PEIM in addition to their even–odd alternations. It is conceivable that a uniaxial orientation process only slightly improves the order correlation lengths in the lateral packing.

Finally, if one plots the layer spacing versus the number of methylene units, a linear relationship can be established as shown in Figure 18. Extrapolation of this linear relationship to $n = 0$ yields a length of 1.28 nm. The slope of this linear relationship is 0.120 nm. These data are in between the cases of PEIM(n=even)s and -(n=odd)s obtained from the fiber patterns but close to the layer spacing of PEIM(n=odd)s as shown in Figure 11. It is surprising that in this case an even–odd alternation cannot be found. A possible explanation may be proposed suggesting that without uniaxial orientation, the layer structure construction in PEIM may not be exactly the same compared to the cases in the fibers. Since the mesogenic group in PEIMs is asymmetric and randomly connected, a relatively broad orientational distribution in PEIMs may exist. Introducing kinks in methylene units may also obscure the layer spacing in PEIMs. However, the detailed reasons are not known at this time.

Morphology and Defects. The morphology and defects of this liquid crystal phase can be observed through SAXS, PLM, and TEM experiments. Figure 19 shows two sets of time-resolved SAXS scattering curves for PEIM(n=10) isothermally kept at (a) 412 K and (b) 422 K. The isothermal temperature was chosen to be slightly below and above the first-order exothermic transition during cooling observed in DSC.[35] For the former case, the transition sequence for PEIM(n=10) is first from the isotropic melt to the smectic A phase during fast cooling to the isothermal temperature and followed by a crystallization. In the initial stage, the scattering peak is broad at around 26 nm as a center long spacing position when the isothermal temperature is at 412 K. After 1.5 min, this scattering peak gradually shifts to higher s values (lower long spacings) and develops to become sharper

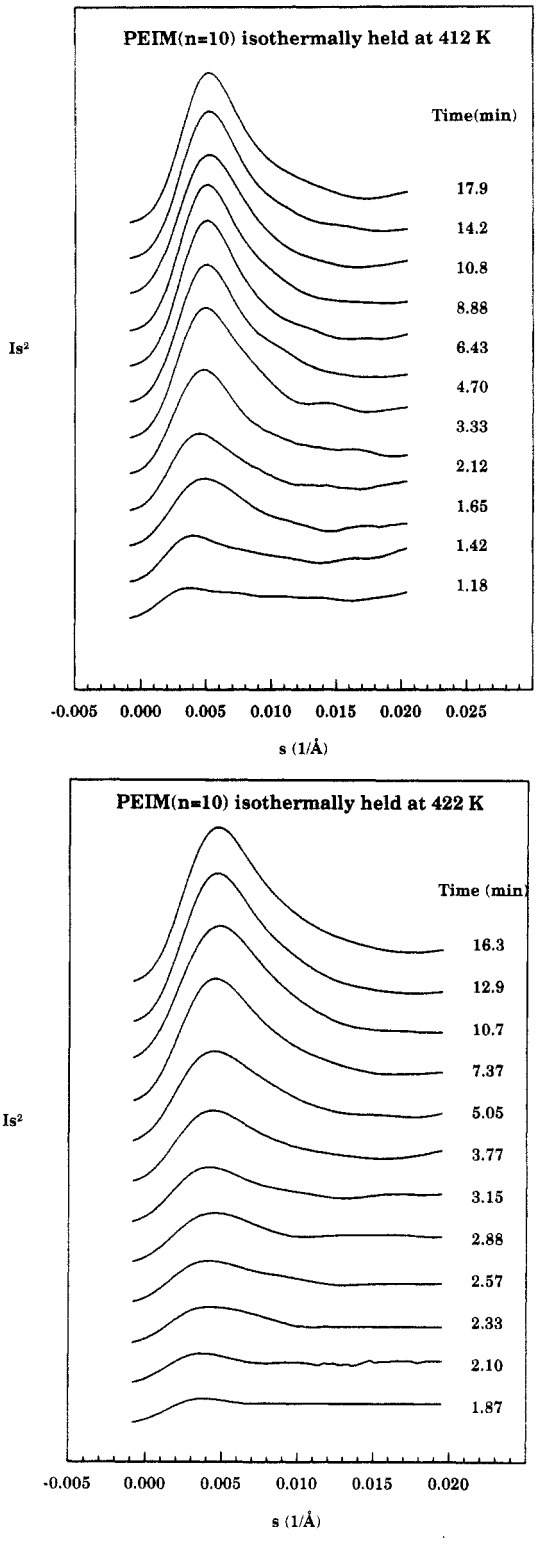

Figure 19. Set of SAXS scattering curves of PEIM(n=10) isothermally kept at 412 K (a, top) and 422 K (b, bottom) at different times.

during the period of time of 4 min. After 6 min, the scattering peak is centered at 20 nm with a constant scattering intensity. It should be noted that PEIM(n=10) completes crystallization at 6 min.[35] The time period of shifting the scattering peak is thus the time for the crystallization process. It is generally difficult to explain the SAXS scattering curves by themselves in a liquid crystal transition which shows initially a long spacing of 26 nm. When combining WAXD structural information with this long spacing, one finds that this initial SAXS scattering peak position for PEIM(n=10) corresponds

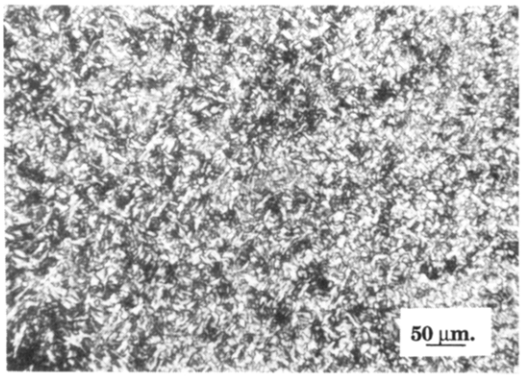

Thread-like Texture of PEIM(n=4) cooled from the isotropic melt

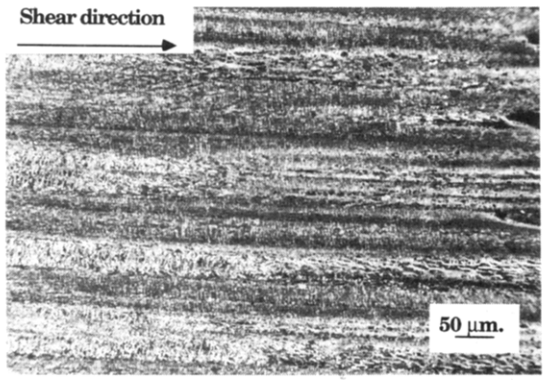

Shear-banded Texture of PEIM(n=4) cooled from the melt

Figure 20. PLM observation of (a, top) liquid crystal texture without shearing; (b, bottom) banded texture of uniaxially sheared PEIM(n=4) samples. The arrow is the shearing direction.

remarkably well to the correlation length of the layer structure shown in Figure 17 (26 nm). Therefore, this long spacing observed from SAXS experiments may be associated with the layer correlation length, which may approximately serve as a domain size in which certain orientational order correlation is retained. Further crystallization leads to the formation of lamellar crystals, and the long spacing in this case represents the size that consisted of a lamellar thickness and two half-sizes of liquid crystal phase region in both sides of the lamella. Interestingly enough, the long spacing after crystallization is only about 6 nm smaller than the orientational correlation length, indicating that the crystal morphology is largely influenced by the previously existing orientational order correlation. On the other hand, the long spacing developed at 422 K for the latter case indicates a crystallization process from the isotropic melt. The long spacing is a constant at 25 nm.

Figure 20 shows under PLM typical morphologies obtained before (Figure 20a) and after the PEIM(n=4) was mechanically sheared at a temperature slightly below the liquid crystal transition temperature (Figure 20b). It is evident that a banded texture can be observed after relaxation, which is perpendicular to the shearing direction. The fact that banded texture appears under an external force field has attracted much attention during 1980s, and this texture has been viewed as a typical liquid crystal polymer pattern.[36-46] A fairly regular banded texture can be formed with a spacer of a few micrometers. Microscopic analysis has shown that, in the banded texture, the director continuously oscillates spatially about the direction imposed by the previous flow.[42,43]

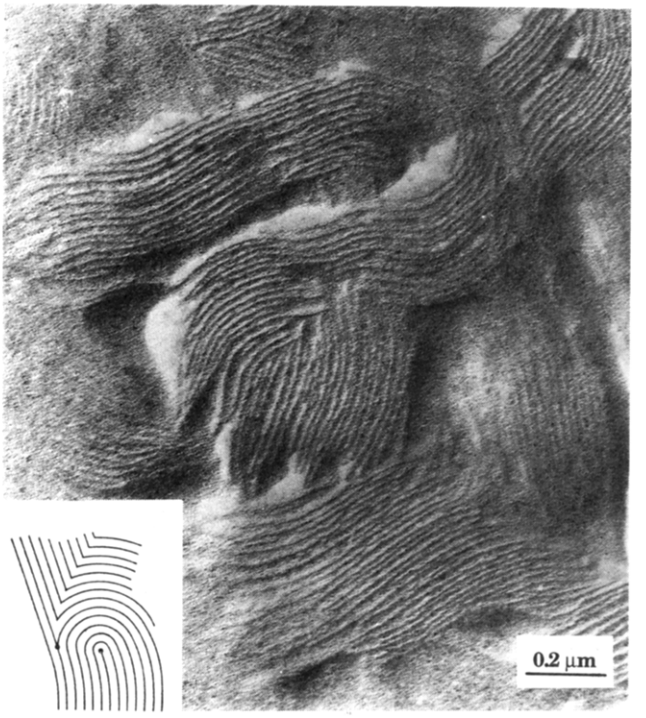

TEM image of Edge Dislocations in PEIM(n=4)

Figure 21. TEM observation of liquid crystal defects consisting of a $+\pi$ and a $-\pi$ disclinations in a uniaxially oriented PEIM-(n=4) sample.

Using the "lamellar decoration method"[25-27] originally developed by Thomas et al., typical liquid crystal defect patterns observed under TEM, as shown in Figures 21 and 22 for PEIM(n=4), were observed. It is evident that the long spacing of 20 nm observed in TEM corresponds well to the SAXS data (Figure 19a). Electron diffraction shows that the chain axis is normal to the long dimension of the lamellae. The trajectories of the chain molecular directions are also included in these figures. Three Frank constants[47] play important roles here. Generally speaking, in a disclination-free sample with a smectic phase, the bend elastic constant (k_{33}) and the twist deformation (k_{22}) should be absent, and only the splay elastic constant (k_{11}) remains. The stratified structure of smectic phase thus imposes certain restrictions on the types of deformation that can take place in it. A compression of the layers requires considerable energy, and therefore, only those deformations that tend to preserve the interlayer spacing are easily possible. The most favorable distortion is thus the bending of the layer, since this involves only a splaying effect and does not affect the layer thickness.[48] The mechanism of the disclination defects formed in a liquid crystal phase has been explained by using the continuun theory[47,49] which is based on the elastic free energy minimization.[50,51] Since the sample preparations of this smectic A phase in PEIMs are nonplanar, the chain molecules are not homeotropic, and therefore, they are not perpendicular to the glass slide surfaces. These defects thus occur in focal conic textures.[52] The different types of defects which are compatible with the layer structure of smectic A phase can be dislocations (edge and screw), disclinations ($+\pi$, $-\pi$, and $+2\pi$), tores, and Dupin cyclides.[53] As pointed out by William and Kleman,[54] who were able to show experimentally tilt walls with dislocations formed during shearing the glass slides in a smectic A phase, the edge dislocation can split into an equivalent pair of $+\pi$ and $-\pi$ disclinations, as shown in Figure 21. On the other hand, the top half of Figure 22 shows a $+\pi$ disclination[47]

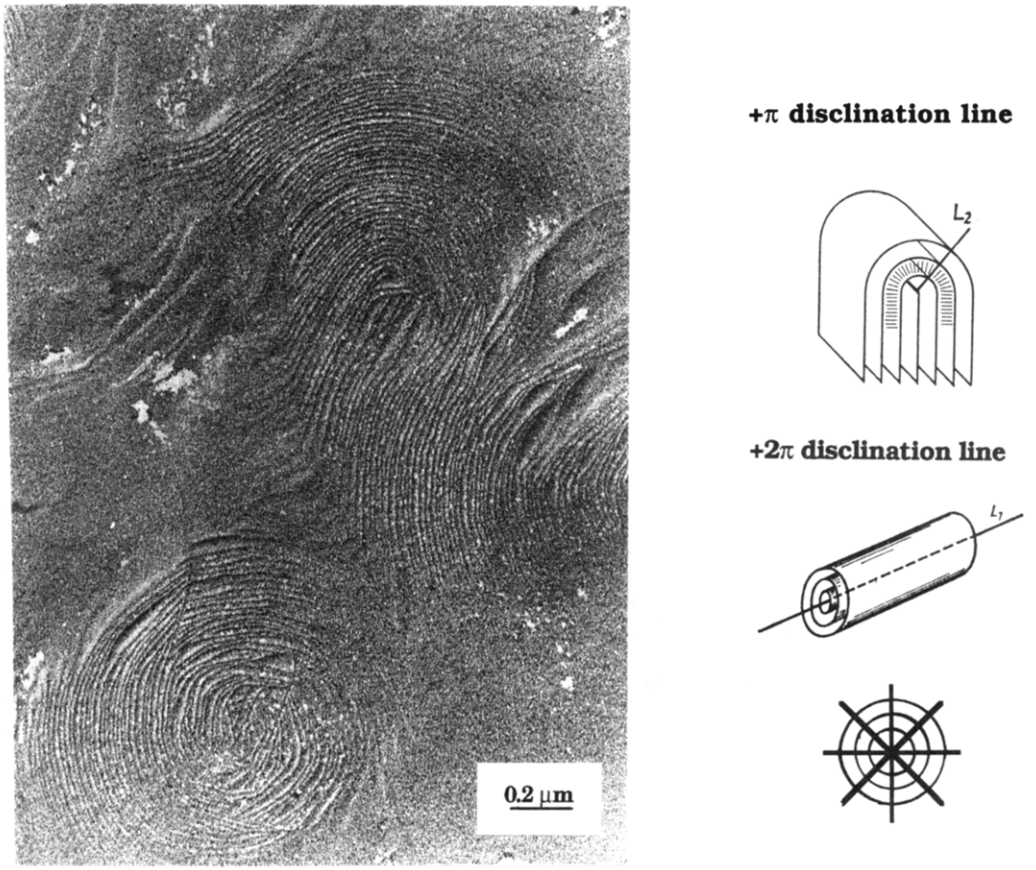

Figure 22. TEM observation of liquid crystal $+\pi$ and $+2\pi$ disclination defects in a uniaxially oriented PEIM(n=4) sample.

with a disclination line (L_2) which is parallel to the view direction of the figure. Namely, the sample preparation cuts this defect in a direction which is perpendicular to the disclination line. It seems that this defect is similar to a $s = +1/2$ wedge disclination in a nematic texture with the elastic anisotropy $\epsilon = 1$,[55-57] where k_{33} is absent and only k_{11} remains. The bottom half of Figure 22 is a $+2\pi$ cylinder disclination which only presents one straight disclination line (L_1). The view direction of this defect is also parallel to this line, and the directions of the chain molecules are oriented with a radial distribution with respect to the line. This topology is somewhat similar to the $s = +1, c = +2\pi$ radial lines in a typical nematic liquid crystal phase. However, the difference between smectic A defects and nematic ones is based on the line singularity versus the core singularity in disclinations.[53] Using high-resolution TEM in very thin films with a thickness of a few ten nanometers, dislocations with multiple Burgers' vectors of a few layers have been observed in main-chain–side-chain mesogen liquid crystal polymers.[58,59] Lamellar crystal decorated defects observed via TEM have also been reported for other thermotropic liquid crystal polymers and copolymers with nematic and smectic liquid crystal textures.[25-27,60-62] It is interesting that for further studies the defect morphology which are associated with three Frank constants changes with molecular weight, chain rigidity, temperature, and strength of external fields.

Conclusion

Combining all the pieces of structural and morphological information obtained through WAXD, SAXS, PLM, and TEM as well as thermal transition behavior from DSC, we can conclude that in PEIMs the liquid crystal phase is monotropic and it possesses a smectic A order. Furthermore, the degree of order and the order correlation of the lateral chain packing and the layer structure show an even–odd alteration. With increasing the number of methylene units, the smectic order is enhanced. Furthermore, the order correlation length along the normal vector of the layer direction (chain direction) is about 1 order of magnitude higher than that long the lateral packing direction. A molecular packing model has been proposed for uniaxially oriented PEIM polymers. The features of this model includes that, first, the layer surface in the uniaxially oriented smectic phase is perpendicular to the orientational direction. Second, the mesogenic group vector in the smectic phase is perpendicular to the layer surface. Third, the methylene units involve a certain degree of kinks, which is higher in PEIM(n=odd)s than that in PEIM(n=even)s.

Acknowledgment. This work was supported by S.Z.D.C.'s Presidential Young Investigator Award from the National Science Foundation (Grant DMR-9157738) and Exxon Education Foundation. Research (in part) was done at the National Synchrotron Light Source (NSLS), Brookhaven National Laboratories, which is supported by the U.S. Department of Energy, Division of Materials Science and Division of Chemical Sciences. R.P. acknowledges the support of Venezuela Technological Institute of Petroleum.

References and Notes

(1) Pardey, R. L.; Zhang, A.-Q.; Gabori, P. A.; Harris, F. W.; Cheng, S. Z. D.; Adduci, J.; Facinelli, V.; Lenz, R. W. *Macromolecules* **1992**, *25*, 5060.
(2) Lehmann, O. *Uber Physikalische Isomerie*; from Keller, H., 1877. History of Liquid Crystals. *Mol. Cryst. Liq. Cryst.* **1973**, *21*, 1.
(3) Volander, D. *The Investigation of Molecular Shape with the Aid of Liquid Crystals*; communication from the Institute of Chemistry of Halle, ADS, 1923.

(4) Percec, V.; Tsuda, Y. *Macromolecules* **1990**, *23*, 4347.
(5) Percec, V.; Yourd, R. *Macromolecules* **1989**, *22*, 524, 3229.
(6) Ungar, G.; Feijoo, J. L.; Keller, A.; Yourd, R.; Percec, V. *Macromolecules* **1990**, *23*, 244.
(7) Ungar, G.; Percec, V.; Zuber, M. *Macromolecules* **1992**, *25*, 1193.
(8) Cheng, S. Z. D.; Yandrasits, M. A.; Percec, V. *Polymer* **1991**, *32*, 1284.
(9) Yandrasits, M. A.; Cheng, S. Z. D.; Zhang, A.-Q.; Cheng, J.-L.; Wunderlich, B.; Percec, V.; *Macromolecules* **1992**, *25*, 2112.
(10) Yandrasits, M. A.; Bruno, K.; Arnold, F. E., Jr.; Cheng, S. Z. D.; Percec, V. *Polym. Adv. Technol.*, in press.
(11) Cheng, J. L.; Wunderlich, B.; Cheng, S. Z. D.; Yandrasits, M. A.; Zhang, A.-Q.; Percec, V. *Macromolecules* **1992**, *25*, 5995.
(12) Yandrasits, M. A. Ph.D. Dissertation, Department of Polymer Science, The University of Akron, Akron, OH, 1991.
(13) Percec, V.; Keller, A. *Macromolecules* **1990**, *23*, 4347.
(14) de Abajo, J.; de la Campa, J. G.; Kricheldorf, H. R.; Schwarz, G. *Makromol. Chem.* **1990**, *191*, 537.
(15) Kricheldorf, H. R.; Huner, R. *Makromol. Chem. Rapid Commun.* **1990**, *11*, 211.
(16) Kricheldorf, H. R.; Domschke, A.; Schwarz, G. *Macromolecules* **1991**, *24*, 1011.
(17) Kricheldorf, H. R.; Jahnke, P. *Eur. Polym. J.* **1990**, *9*, 1009.
(18) Kricheldorf, H. R.; Schwarz, G.; de Abajo, J.; de la Campa, J. G. *Polymer* **1991**, *32*, 942.
(19) Kricheldorf, H. R.; Huner, R. *J. Polym. Sci., Polym. Chem.* **1992**, *30*, 337.
(20) Noel, C. In *Polymeric Liquid Crystals*; Blumstein, A., Ed.; Plenum: New York, 1985; pp 21–63.
(21) Ober, C. K.; Jin, J. I.; Lenz, R. W. *Makromol. Chem. Rapid Commun.* **1983**, *4*, 49.
(22) Roviello, A.; Sirigu, A. *Gazz. Chim. Ital.* **1980**, *110*, 403.
(23) Frosini, P.; Marchetti, A. *Makromol. Chem. Rapid Commun.* **1982**, *3*, 795.
(24) Thierry, A.; Skoulios, A.; Lang, G.; Forestier, S. *Mol. Cryst. Liq. Cryst., Lett. Sect.* **1978**, *41*, 125.
(25) Thomas, E. L.; Wood, B. A. *Faraday Discuss. Chem. Soc.* **1985**, *79*, 229.
(26) Wood, B. A.; Thomas, E. L. *Nature* **1986**, *324*, 655.
(27) Hudson, S. D.; Vezie, D.; Thomas, E. L. *Makromol. Chem. Rapid Commun.* **1990**, *11*, 657.
(28) Blumstein, A.; Thomas, O. *Macromolecules* **1982**, *15*, 1264.
(29) Blumstein, R. B.; Stickles, E. M.; Blumstein, A. *Mol. Cryst. Liq. Cryst., Lett. Sect.* **1982**, *82*, 205.
(30) Blumstein, R. B.; Blumstein, A. *Mol. Cryst. Liq. Cryst.* **1988**, *165*, 361.
(31) de Gennes, P.-G. *Mol. Cryst. Liq. Cryst., Lett. Sect.* **1984**, *102*, 95.
(32) Abe, A. *Macromolecules* **1984**, *17*, 2280.
(33) Yoon, D. Y.; Bruckner, S. *Macromolecules* **1985**, *18*, 651.
(34) de Vries, A. *Pranama Suppl.* **1975**, *1*, 93; see also, Tsukruk, V. *Makromol. Chem. Makromol. Symp.* **1991**, *44*, 109.
(35) Pardey, R. Ph.D Dissertation, Department of Polymer Science, The University of Akron, Akron, OH, 1993.
(36) Kiss, G.; Porter, R. S. *Mol. Cryst. Liq. Cryst.* **1980**, *60*, 267.
(37) Donald, A. M.; Viney, C.; Windle, A. H. *Polymer* **1983**, *24*, 155.
(38) Viney, C.; Donald, A. M.; Windle, A. H. *J. Mater. Sci.* **1983**, *18*, 1137.
(39) Shimamura, K. *Makromol. Chem. Rapid Commun.* **1983**, *4*, 107.
(40) Graziano, D. J.; Mackley, M. R. *Mol. Cryst. Liq. Cryst.* **1984**, *106*, 73.
(41) Hu, S.; Xu, M.; Li, J.; Qian, B.; Wang, X.; Lenz, R. W. *J. Polym. Sci., Polym. Phys. Ed.* **1985**, *23*, 2387.
(42) Viney, C.; Windle, A. H. *Polymer* **1986**, *27*, 1325.
(43) Navard, P.; Zachariades, A. E. *J. Polym. Sci., Polym. Phys. Ed.* **1987**, *25*, 1089.
(44) Fincher, C. R. *Mol. Cryst. Liq. Cryst.* **1988**, *155*, 559.
(45) Marsano, E.; Capareto, L.; Ciferri, A. *Mol. Cryst. Liq. Cryst.* **1988**, 158, 267.
(46) Maffettone, P. L.; Grizzuti, N.; Marrucci, G. *Liq. Cryst.* **1989**, *4*, 385.
(47) Frank, F. C. *Faraday Discuss. Soc.* **1958**, *25*, 19.
(48) Chandrasekhar, S. In *Polymer, Liquid Crystals, and Low-Dimensional Solids*; March, N., Tosi, M., Eds; Plenum: New York, 1984.
(49) Nehring, J.; Saupe, A. *Faraday Trans. Chem. Soc.* **1972**, *68*, 1.
(50) de Gennes, P.-G. *The Physics of Liquid Crystals*; University Press: Oxford, 1974.
(51) de Gennes, P.-G. *J. Phys. (Paris)* **1969**, *30*, 65.
(52) Friedel, G.; Grandjean, F. *Bull Soc. Fr. Miner.* **1910**, *33*, 192, 409.
(53) Demus, D.; Richter, L. *Textures of Liquid Crystals*; Weinheim, New York, 1978.
(54) William, C. E.; Kleman, M. *J. Phys., Colloq.* **1975**, *36*, 315.
(55) Dzyaloshinkii, I. E. *Sov. Phys. JETP* **1970**, *31*, 773.
(56) Hudson, S. D.; Thomas, E. L. *Phys. Rev. Lett.* **1989**, *62*, 1993.
(57) Hudson, S. D.; Thomas, E. L. *Chemtracts: Macromol. Chem.* **1991**, *2*, 73.
(58) Voigt-Martin, I. G.; Durst, H.; Reck, B.; Rinsdorf, H. *Macromolecules* **1988**, *21*, 1620.
(59) Voigt-Martin, I. G.; Durst, H. *Macromolecules* **1989**, *22*, 168.
(60) Mazelet, G.; Keleman, M. *J. Mater. Sci.* **1988**, *23*, 3055.
(61) Windle, A. H.; Viney, C.; Gulombok, R.; Donald, A. M.; Mitchell, G. R. *Faraday Discuss. R. Chem. Soc.* **1985**, *79*, 55.
(62) Shiwaku, T.; Nakai, A.; Hasegawa, H.; Hashimoto, T. *Macromolecules* **1990**, *23*, 1590.